Journal of Nuclear Materials 396 (2010) 218–222

Contents lists available at ScienceDirect

Journal of Nuclear Materials

journal homepage: www.elsevier.com/locate/jnucmat

First-principles study of UC_2 and U_2C_3

Hongliang Shi [a,b], Ping Zhang [a,c,*], Shu-Shen Li [b], Baotian Wang [d], Bo Sun [a]

[a] LCP, Institute of Applied Physics and Computational Mathematics, P.O. Box 8009, Beijing 100088, People's Republic of China
[b] State Key Laboratory for Superlattices and Microstructures, Institute of Semiconductors, Chinese Academy of Sciences, P.O. Box 912, Beijing 100083, People's Republic of China
[c] Center for Applied Physics and Technology, Peking University, Beijing 100871, People's Republic of China
[d] Institute of Theoretical Physics and Department of Physics, Shanxi University, Taiyuan 030006, People's Republic of China

ARTICLE INFO

Article history:
Received 29 June 2009
Accepted 13 November 2009

Keywords:
First-principle calculation
GGA+U
Elastic constants
Chemical bonding
Valence state

ABSTRACT

The electronic structure and mechanical properties of UC_2 and U_2C_3 have been systematically investigated using first-principles calculations by the projector-augmented-wave (PAW) method. Furthermore, in order to describe precisely the strong on-site Coulomb repulsion among the localized U 5*f* electrons, we adopt the generalized gradient approximation +*U* formalisms for the exchange-correlation term. We show that our calculated structural parameters and electronic properties for UC_2 and U_2C_3 are in good agreement with the experimental data by choosing an appropriate Hubbard $U = 3$ eV. As for the chemical bonding nature, the contour plot of charge density and total density of states suggest that UC_2 and U_2C_3 are metallic mainly contributed by the 5*f* electrons, mixed with significant covalent component resulted from the strong C—C bonds. The present results also illustrate that the metal–carbon (U—C) bonding and the carbon–carbon covalent bonding in U_2C_3 are somewhat weaker than those in UC_2, leading to the weaker thermodynamic stability at high temperature as observed by experiments.

1. Introduction

Uranium carbides UC, UC_2 and U_2C_3 are the three intermediate phases observed in the uranium–carbon system [1]. Among these carbides, UC has been studied extensively like other NaCl-type metallic actinide compounds [2,3]. The melting points and stiffness of UC is very high. However, for uranium dicarbide UC_2 and uranium sesquicarbide U_2C_3, only some experimental data on structural parameters and thermodynamics properties can be obtained [4–6]. As the important nuclear materials, they have great technological importance because of their applications in the nuclear reactor. Therefore, a systematic investigation of the electronic structures, chemical bonding, and mechanical properties of UC_2 and U_2C_3 from theoretical viewpoint is indispensable to their applications in the nuclear industry.

The elemental actinide metals and their compounds exhibit many exotic behaviors because of the complex character of the 5*f* electrons. In actinide compounds, part of the 5*f* electrons are neither well localized nor completely itinerant [7]. The localization of the 5*f* electrons and strong on-site Coulomb repulsion between them play an important role. Traditional density-functional schemes that apply the local density approximation (LDA) or the generalized gradient approximation (GGA) underestimate the strong on-site Coulomb repulsion of the U 5*f* electrons and, consequently, fail to capture the electronic localization effects. To overcome the drawback mentioned above, the so-called LDA + *U* or GGA + *U* scheme, which modifies the intra-atomic Coulomb interaction by turning on the Hubbard *U* parameter [8,9], is an effective approach to realize it. As for the value of *U* parameter, it is often fitted to reproduce a certain set of experimental lattice constant, band gap and other structural parameters.

In this work, we use the GGA + *U* schemes due to Dudarev et al. [10] to investigate the lattice parameter, electronic structure and elastic constants of UC_2 and U_2C_3. We show that by choosing an appropriate Hubbard *U* parameter around 3 eV, the structural parameters and electronic properties for UC_2 and U_2C_3 can be well reproduced, which are in good agreement with the experimental data. The chemical bonding properties of UC_2 and U_2C_3 are also investigated and our results show that they both exhibit metallic bonding accompanying significant covalent component.

This paper is organized as follows. The details of our calculations are described in Section 2 and in Section 3, we present and discuss the results. In Section 4, we summarize our investigations.

2. Details of calculation

Our first-principles calculations are based on the density functional theory (DFT) and the Vienna ab initio simulation package (VASP) [11] using the GGA for the exchange-correlation potential [12]. The electron and core interactions are included using the frozen-core projected augmented wave (PAW) approach which combines the accuracy of augmented-plane-wave methods with the

---

* Corresponding author. Address: LCP, Institute of Applied Physics and Computational Mathematics, P.O. Box 8009, Beijing 100088, People's Republic of China. Tel.: +86 10 82305133.
E-mail address: zhang_ping@iapcm.ac.cn (P. Zhang).

0022-3115/$ - see front matter © 2009 Elsevier B.V. All rights reserved.
doi:10.1016/j.jnucmat.2009.11.009

efficiency of the pseudopotential approach [13]. The U 5*f*, 6*s*, 6*p*, 6*d* and 7*s* as well as the Carbon 2*s* and 2*p* electrons are explicitly treated as valence electrons. The electron wave function is expanded in plane waves up to a cutoff energy of 500 eV. The strong on-site Coulomb repulsion among the localized U 5*f* electrons is described by using the formalism formulated by Dudarev et al. [10]. In this scheme, only the difference between the spherically averaged screened Coulomb energy U and the exchange energy J is important for the total LDA (GGA) energy functional. Thus, in the following we label them as one single parameter U for brevity. Our previous work showed that the calculated electronic structures and mechanical properties for uranium carbide (UC) agree well with the experimental values by choosing the Hubbard U parameter around 3 eV [14]. Therefore, we also use this value for all our following calculations for UC_2 and U_2C_3.

In our calculation, we study UC_2 in its low temperature α phase of the CaC_2-type structure with space group $I4/mmm$ (No. 139) and U_2C_3 in its Pu_2C_3-type structure with space group $I\bar{4}3d$ (No. 220) [5]. For UC_2, the $11 \times 11 \times 11$ Monkhorst–Pack *k*-point mesh [9] is used for Brillouin-zone integration. For U_2C_3, the $8 \times 8 \times 8$ Monkhorst–Pack *k*-point mesh [15] is used. In order to get the electronic density of states (DOS), we use the $13 \times 13 \times 13$ (196 irreducible *k* points) and $10 \times 10 \times 10$ (44 irreducible *k* points) Monkhorst–Pack *k*-point meshes for UC_2 and U_2C_3, respectively. For the relaxation in calculating the elastic constants, the Brillouin-zone integration was performed using the Methfessel–Paxton scheme [16] and the geometries were optimized by minimizing the quantum mechanical forces acting on the atoms. For the total energy and DOS calculations, the tetrahedron method with Blöchl corrections [17] is used for the Brillouin-zone integration.

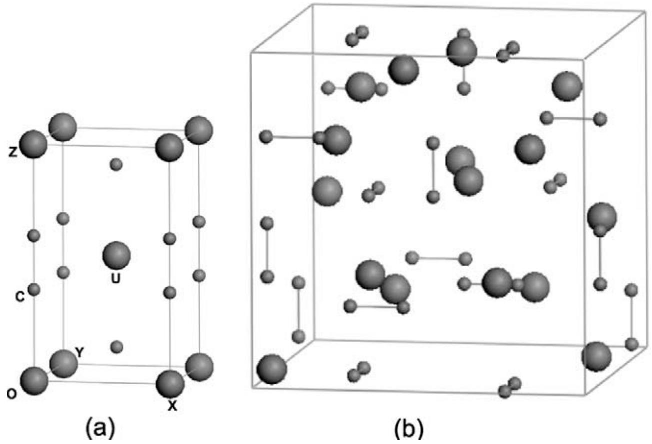

Fig. 1. (a) Unit cell of UC_2 with CaC_2-type structure (body centered tetragonal) and (b) unit cell of U_2C_3 with Pu_2C_3-type structure (body centered cubic). The large and small spheres denote U and C atoms, respectively.

Table 1
Calculated lattice constants a_0 (nm) and interatomic distances (nm) for UC_2 by the GGA + U scheme with Hubbard U = 3 eV.

GGA	This work	Other work	Expt.	Expt.
a_0 (nm)	0.3533	0.3524[a]	0.3516[b]	0.3509 ± 0.0003[c]
c_0 (nm)	0.6044	0.5946[a]	0.6003 [b]	0.5980 ± 0.0005[c]
z	0.386	0.3860[a]	0.388[b]	0.388 ± 0.002[c]
d (C—C) (nm)	0.1377	0.1312[a]		0.134[c]
d (U—2C) (nm)	0.2333	0.2317[a]		0.2325[c]
d (U—8C) (nm)	0.2591	0.2577[a]		0.259[c]

[a] Previous theoretical values from Ref. [18].
[b] Experimental values from Ref. [4].
[c] Experimental values from Ref. [5].

3. Results and discussions

3.1. Atomic and electronic structure of UC_2

UC_2 crystallizes in the body centered tetragonal structure, with spacegroup $I4/mmm$, U on site 2*a* (0, 0, 0) and C on site 4*e* (0, 0, *z*), where *z* is one internal parameter. The crystal structure of UC_2 is shown in Fig. 1a. Our calculated atomic structural parameters, such as lattice constants a_0, c_0, internal parameter *z*, and interatomic distances, are collected in Table 1 together with the corresponding experimental values and other theoretical data. Our calculated a_0 (c_0) is 0.3533 (0.6044) nm, which is consistent well with the experimental data of 0.3516 (0.6003) nm [4] and 0.3509 ± 0.0003 (0.5980 ± 0.0005) nm [5]. The present calculated parameter *z* is 0.386, which is also in excellent with the experimental measurement values of 0.388 [4] and 0.388 ± 0.002 [5]. As for the interatomic distances, one can see that all the experimental values are reproduced well. Note that the present *d* (C—C) 0.1377 nm is a little larger than the theoretical value 0.1312 nm obtained by the ultrasoft pseudopotential methods [18].

The total DOS per primitive cell for UC_2 is shown in Fig. 2a. For more clear illustration, the orbital-resolved partial DOS for U and C atoms are also shown, Fig. 2b for one U atom and Fig. 2c for two C atoms. From Fig. 2 one can see the following prominent features: (i) UC_2 is metallic, which is mainly contributed by U 5*f* electrons at the Fermi energy. This is similar to the system of UC; (ii) U 5*f* and 6*d* states hybridize with C 2*s* and 2*p* states in the energy range from −8 to 2 eV. According to our following charge distribution and valence state analysis, U ions are partially ionized. Therefore, part of the 5*f* electrons contribute for the metallic bonding and part of the 5*f* electrons transfer to C 2*p* states and into the interstitial zone and (iii) the sp^2 hybridization between C atoms still exists along the (001) direction. We summarize the DOS of the two Carbon atoms in the per primitive cell since they are identical. Surprisingly, the C—C bond of 0.1377 nm in UC_2 is remarkably shorter than that of 0.142 nm within the usual graphite layer. The reason is due to the strong electrostatic interaction between the U ion located in the body centered site and the eight C ions. Because of the strong sp^2 hybridization in the short C—C bonds, the resulting covalent property is very strong as discussed in the following.

In order to obtain further understanding of the electronic structure and bonding character for UC_2, the contour of the charge density in the (110) plane containing two nearest C—C bonds and two U atoms is plotted in Fig. 3. It is clear that the charge density is larger than 190 e/nm^3 in most of the interstitial region and some closed contour exists between the U and C atoms, especially between the nearest C and C atoms. These results suggest that the bonding nature in UC_2 is mainly metallic accompanying some significant covalent component. The distribution of charge density around the U atom is nearly spherical, while for the nearest C—C atoms, the charge density distribution is largely deformed toward their bonds. Therefore, it is easy to decide U ionic radius and valence state. In this work, we determine the ionic radius according to the minimum value of charge density along the nearest U—C bond. The present calculated ionic radius for U ion is 0.130 nm and there are 10.30 electrons around U ions within this radius. Therefore, U ion is partially ionized and can be represented as $U^{3.7+}$.

As for the mechanical properties, which have not been studied in previous theoretical reports. We calculate the elastic constants for UC_2 from total energy variation response to small strains. In our calculation the strain δ is varied in steps of 0.006 from −0.036 to 0.036. For the tetragonal structure, there are six independent elastic constants $C_{11}, C_{12}, C_{13}, C_{33}, C_{55}$ and C_{66}. The calculated results are listed in Table 2. Our results show that the

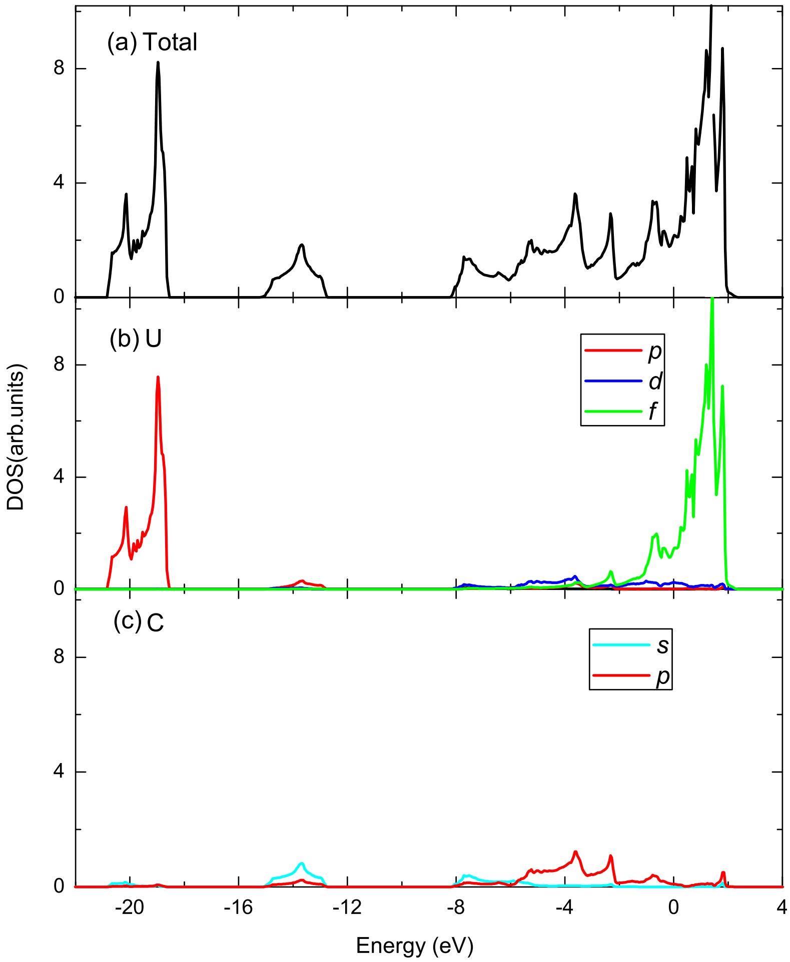

Fig. 2. Total density of states for UC_2 and projected density of states for one U nd two C atoms. The Fermi energy is set to zero.

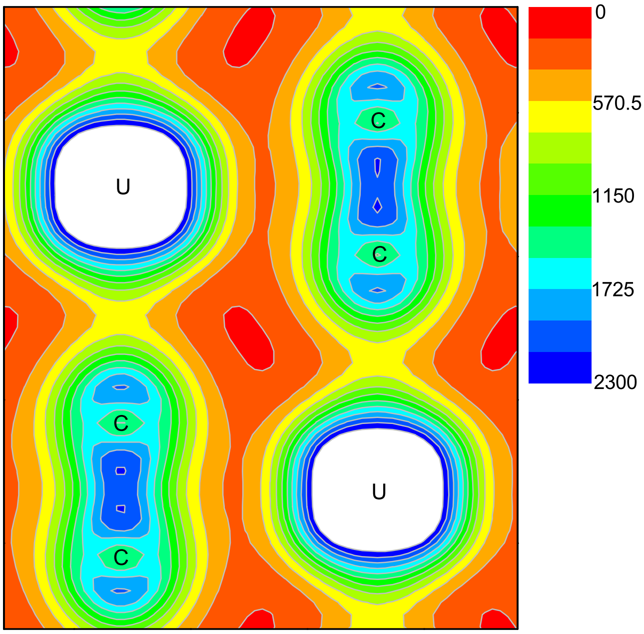

Fig. 3. Contour plot of the charge density for UC_2 in the (1 1 0) plane. The contour lines are plotted form 0.0 to 2300 by the interval of 575.0 e/nm^3.

Table 2
Calculated elastic constants (GPa) and bulk modulus *B* (GPa) for UC_2 by the GGA + *U* scheme with Hubbard *U* = 3 eV.

GGA	C_{11}	C_{12}	C_{13}	C_{33}	C_{55}	C_{66}	B
Present	292	154	58	512	46	143	180.5
Expt.							216[a]

[a] Experimentally measured values from Ref. [4].

elastic constants well obey the mechanical stability criteria listed in below [19]:

$$C_{11} > 0, C_{33} > 0, C_{44} > 0, C_{66} > 0,$$
$$(C_{11} - C_{12}) > 0, (C_{11} + C_{33} - 2C_{13}) > 0,$$
$$[2(C_{11} + C_{12}) + C_{33} + 4C_{13}] > 0. \quad (1)$$

Therefore, the body centered tetragonal UC_2 is mechanical stable.

After obtaining the elastic constants, we can calculate the bulk modulus from the Voigt–Reuss–Hill (VRH) approximation [20–22]. Under Voigt [20] and Reuss [21] approximation, the bulk modules and shear modulus can be expressed as:

$$B_V = (1/9)[2(C_{11} + C_{12}) + C_{33} + 4C_{13}], \quad (2)$$

$$G_V = (4C_{11} - 2C_{12} + 2C_{33} - 4C_{13} + 12C_{44} + 6C_{66})/30, \quad (3)$$

$$B_R = [(C_{11} + C_{12})C_{33} - 2C_{13}^2]/[C_{11} + C_{12} + 2C_{33} - 4C_{13}], \quad (4)$$

and

$$G_R = 15\{[18B_v/(C_{11}C_{33} + C_{12}C_{33} - 2C_{13}^2)] + [6/(C_{11} - C_{12})] + (6/C_{44}) + (3/C_{66})\}^{-1}, \quad (5)$$

respectively. The present B_V, B_R, G_V and G_R are 182, 179, 102 and 60 GPa, respectively. Based on Hill approximation [22], the bulk

Table 3
Calculated and experimental lattice constants a_0 (nm) and bulk modules B (GPa) for U_2C_3 by the GGA + U scheme with Hubbard U = 3 eV.

	a_0	d (C—C)	d (U—3C)	d (U—3C)	d (U—3C)
Present	0.8097	0.1438	0.2438	0.2567	0.2785
Expt.	0.80885	0.1295	0.250	0.256	0.282

modulus B, are arithmetic averages of Voigt and Reuss elastic modulus, from which Poisson's ratio υ is given by

$$\upsilon = \frac{3B - 2G}{2(3B + G)}$$

Therefore, using above functions the present bulk modulus B is 180.5 GPa, which is somewhat underestimated compared with the experimental value of 216 GPa [4]. The calculated Poisson's ratio υ is 0.30, which is well within the range (from 0.25 to 0.45) for typical metals.

3.2. Atomic and electronic structure of U_2C_3

Uranium sesquicarbide U_2C_3, similar to the rare earth sesquicarbides, crystallizes in the body centered cubic Pu_2C_3 structure. U and C locate at the sites of 16c (u, u, u) and 24d (υ, 0, 0.25), respectively, where u and υ are the two internal parameters. For the atomic structural parameters, our calculated lattice constant is 0.8097 nm, which is obtained by fitting the Murnaghan equation of state [23] and well accords with the experimental value of 0.80885 ± 0.00005 nm [5]. As for internal parameter u and υ, the present results are 0.047 and 0.286, comparable well with the experimental values of 0.050 ± 0.003 and 0.28, respectively [5]. The bond distances of C—C, U—C, and corresponding experimental values [5] are also listed in Table 3. All these results indicate that the GGA + U scheme with U = 3 eV can effectively describe the atomic structural parameters. Based on this, we discuss the DOS, band structure, charge density, and mechanical properties of U_2C_3 in the following. The total DOS and band structure are plotted in Fig. 4. In these figures, the Fermi energy level is set to zero. One can see that U_2C_3 is also metallic. This confirms that the three uranium carbides are all metallic and the metallicity is mainly contributed by U 5f electrons. From the band structure, one can see that the bands derived from U 6p orbitals cover from −21.0 to −18.7 eV. Then a very narrow manifold of bands mainly contributed by C 2s and 2p electrons is followed. The U 5f, U 6d and C 2p resulting bands cover from −8.7 to 0.8 eV near the Fermi level. As for the valence state of U ion, our calculation shows it can be represented as $U^{+3.2}$ with ionic radius of 0.136 nm. Therefore, the U ions in U_2C_3 are ionized somewhat less than U ions in UC_2.

The C—C dimers with short bond lengths is a typical character in the body centered cubic sesquicarbides [24]. Our calculated C—C bond length is 0.1438 nm which is a little larger than the nearest C—C bond length 0.1377 nm in UC_2, suggesting somewhat weaker C—C covalency in the former. In order to test this, the charge density along the nearest C—C bond together with the U—C bond for UC_2 and U_2C_3 is plotted in Fig. 5. One can see that the density in the middle zone along the C—C bond for UC_2 is larger than that for U_3C_2. This confirms our above speculation that the covalency existing between the C—C bond is stronger in UC_2. Note that the corresponding minimum values of the charge density are 2090 and 1830 e/nm^3 for C—C bonds of UC_2 and U_2C_3, respectively. This further illustrates that the C—C bond is typical covalent bond in

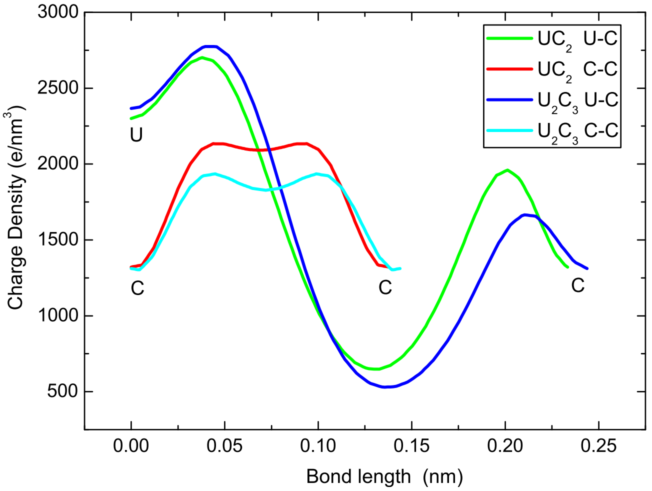

Fig. 5. The charge density distribution along the nearest U—C and C—C bonds for UC_2 and U_2C_3, respectively.

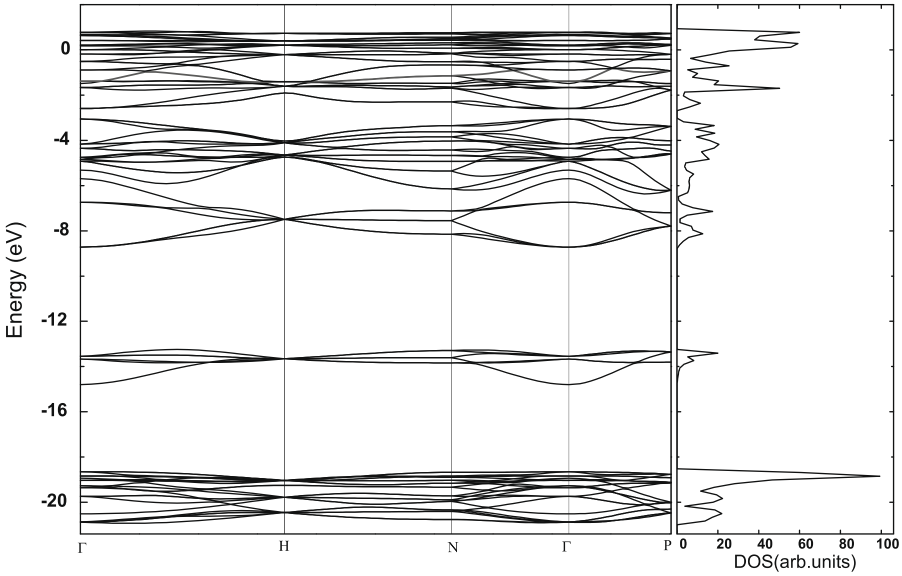

Fig. 4. Calculated band structure and total density of states for U_2C_3. The Fermi energy is set to zero.

Table 4
Calculated elastic constants and bulk modulus for U_2C_3 by the GGA + *U* scheme with Hubbard *U* = 3 eV.

GGA	C_{11}	C_{12}	C_{44}	B
(GPa)	383	121	91	208

these two uranium carbides compared with Si typical covalent bond of 700 e/nm^3. As for the U—C bonds, the corresponding minimum values are 650 and 530 e/nm^3 for UC_2 and U_2C_3, respectively. Note that some covalent component exists in the U—C bonds for UC_2 since a few closed contour appears between them as aforementioned. Therefore, the above results clearly and consistently demonstrate that strong covalent component also exists in the C—C bonds in U_2C_3 and the metal–carbon (U—C) bonding is weaker than that in UC_2. Furthermore, the weaker U—C bonds in U_2C_3 is also illustrated by its decomposition into UC_2 and graphite at high temperature as observed by experiments [6].

The calculated three independent elastic constants for cubic U_2C_3 are collected in Table 4 and the results of C_{11}, C_{12} and C_{44} are 383, 121 and 91 GPa, respectively. The bulk modulus *B* evaluated from the elastic constants is 208 GPa. Note that the bulk modules *B* obtained by fitting the Murnaghan equation of state [23] is 198 GPa. Therefore, these results obtained by two different methods are consistent well with each other, suggesting that the calculations are self-consistent. For U_2C_3, the Poisson's ratio v is 0.28 within the range of the typical metal. Furthermore, interesting, we find that for the three uranium carbides UC, UC_2 and U_2C_3, the Poisson's ratio decreases, i.e., from 0.32 [14], 0.30 to 0.28.

4. Conclusions

In summary, we have reported theoretically the investigations of the structural, electronic, and mechanical properties of UC_2 and U_2C_3 using first-principles calculations based on DFT within GGA + *U* frameworks. The lattice constants, interatomic distances, and bulk modules are well reproduced and theses results obtained at Hubbard *U* = 3 eV with GGA scheme are reasonable compared with the experimental values. The electronic properties show that the two uranium carbides are both metallic mainly contributed by U 5*f* electrons. We have also calculated the elastic constants for UC_2 and U_2C_3 and our results well obey the mechanical stability criteria. As for the Poisson's ratio, the calculated results are 0.30 and 0.28 for UC_2 and U_2C_3, respectively, which are well within the range for the typical metal. Further analysis demonstrate that the chemical bonding in the two compounds has significant covalent component resulted from the stronger C—C interaction with short bond length. The metal–carbon (U—C) bond in U_2C_3 is weaker compared with other uranium carbides. According to our valence state calculation, the U ions in UC_2 and U_2C_3 can be represented as $U^{3.7+}$ and $U^{3.2+}$, respectively. We expect our results are helpful for further studies of the properties of uranium carbides.

Acknowledgments

This work was supported by the Foundations for Development of Science and Technology of China Academy of Engineering Physics.

References

[1] P.Y. Chevalier, E. Fischer, J. Nucl. Mater. 288 (2001) 100.
[2] S.C. Goyal, A.K. Goyal, Phys. Status Solidi (b) 77 (1976) 639.
[3] J. Trygg, J.M. Wills, M.S.S. Brooks, B. Johansson, O. Eriksson, Phys. Rev. B 52 (1995) 2496.
[4] J.-P. Dancausse, S. Heathman, U. Benedict, L. Gerward, J. Staun Olsen, F. Hulliger, J. Alloy. Compd. 191 (1993) 309.
[5] B.A.E. Austin, Acta. Cryst. 12 (1959) 159.
[6] V.V. Akhachinskii, S.N. Bashlykov, UDC 621.039.542.3.
[7] P. Erdös, John M. Robinson, The Physics of Actinide Compounds, Plenum, New York, 1983, pp. 4.
[8] V.I. Anisimov, J. Zaanen, O.K. Anderson, Phys. Rev. B 44 (1991) 943.
[9] V.I. Anisimov, I.V. Solovyev, M.A. Korotin, M.T. Czyzyk, G.A. Sawatzky, Phys. Rev. B 48 (1993) 16929.
[10] S.L. Dudarev, G.A. Dudarev, S.Y. Savrasov, C.J. Humphreys, A.P. Sutton, Phys. Rev. B 57 (1998) 1505.
[11] G. Kresse, J. Hafner, Phys. Rev. B 48 (1993) 13115.
[12] Y. Wang, J.P. Perdew, Phys. Rev. B 44 (1991) 13298.
[13] G. Kresse, D. Joubert, Phys. Rev. B 59 (1999) 1758.
[14] H. Shi, P. Zhang, S.-S. Li, B. Sun, B. Wang, Phys. Lett. A 373 (2009) 3577.
[15] H.J. Monkhorst, J.D. Pack, Phys. Rev. B 13 (1972) 5188.
[16] M. Methfessel, A.T. Paxton, Phys. Rev. B 40 (1989) 3616.
[17] P.E. Blöchl, O. Jepsen, O.K. Andersen, Phys. Rev. B 49 (1994) 16223.
[18] Chris J. Pickard, Bjoön Winkler, Roger K. Chen, M.C. Payne, M.H. Lee, J.S. Lin, J.A. White, V. Milman, D. Vanderbilt, Phys. Rev. Lett. 85 (2000) 5122.
[19] Z. Wu, E. Zhao, H. Xiang, X. Hao, X. Liu, J. Meng, Phys. Rev. B 76 (2007) 054115.
[20] W. Voigt, Lehrburch der Kristallphysik, Teubner, Leipzig, 1928.
[21] A. Reuss, Z. Angew, Math. Mech. 9 (1929) 49.
[22] R. Hill, Phys. Soc. Lond. 65 (1952) 350.
[23] F.D. Murnaghan, Proc. Natl. Acad. Sci. USA 30 (1944) 244.
[24] D.J. Singh, I.I. Mazin, Phys. Rev. B 70 (2004) 052504.